Available online at www.sciencedirect.com
SCIENCE DIRECT®
Journal of Sound and Vibration 260 (2003) 611–635
JOURNAL OF SOUND AND VIBRATION
www.elsevier.com/locate/jsvi

Vehicle–passenger–structure interaction of uniform bridges traversed by moving vehicles

E. Esmailzadeh[a], N. Jalili[b,*]

[a] Department of Mechanical Engineering, Sharif University of Technology, P.O. Box 11365-9567, Tehvan, Iran
[b] Robotics and Mechatronics Laboratory, Department of Mechanical Engineering, Clemson University, Clemson, SC 29634-0921, USA

Received 9 June 2001; accepted 29 April 2002

Abstract

An investigation into the dynamics of vehicle–occupant–structure-induced vibration of bridges traversed by moving vehicles is presented. The vehicle including the driver and passengers is modelled as a half-car planar model with six degrees-of-freedom, and the bridge is assumed to obey the Euler–Bernoulli beam theory with arbitrary conventional boundary conditions. Due to the continuously moving location of the variable loads on the bridge, the governing differential equations become rather complicated. The numerical simulations presented here are for the case of vehicle travelling at a constant speed on a uniform bridge with simply supported end conditions. The relationship between the bridge vibration characteristics and the vehicle speed is rendered, which yields into a search for a particular speed that determines the maximum values of the dynamic deflection and the bending moment of the bridge. Results at different vehicle speeds demonstrate that the maximum dynamic deflection occurs at the vicinity of the bridge mid-span, while the maximum bending moment occurs at $\pm 20\%$ of the mid-span point. It is shown that one can find a critical speed at which the maximum values of the bridge dynamic deflection and the bending moment attain their global maxima.

1. Introduction

The dynamic behavior of bridge structures subjected to moving loads or moving masses has been a topic of interest for well over a century. Interest in this problem was originated, in civil engineering, for the design of railway tracks and bridges and, in mechanical engineering, for the trolleys of overhead cranes that move on their girders as well as in the machining processes. The

*Corresponding author.
E-mail address: jalili@clemson.edu (N. Jalili).

0022-460X/03/$ - see front matter
PII: S0022-460X(02)00960-4

problem arose from the observations that as a bridge structure is subjected to moving vehicles and trains, the dynamic transversal deflection as well as the stresses could become significantly higher than those for the static loads could.

Two early interesting contributions in this area are due to Stokes [1] and Willis [2] for the cases of a pulsating load passing over a beam and for the analysis of trains crossing a bridge. Timoshenko [3] presented the classical solution of a beam subjected to a constant moving load, while Ayre et al. [4] presented the exact solution of the resulting partial differential equation for the dynamic response of a symmetrical two-span beam subjected to moving load. A complete solution of the problem of the dynamic behavior of a prismatic bar acted upon by a load of constant magnitude and moving with a constant velocity was presented by Krylov [5,6] and Inglis [7].

With the large increase in the proportion of heavy and articulated trucks and high-speed vehicles in highway and railway traffic, the dynamic interaction problem between vehicles and bridge structures attracted much attention during the last three decades. Early models adopted to simulate bridge–vehicle interaction normally considered simply supported beams with a single, lumped load moving at constant speed along its span. These models evolve from the original works initiated by Fryba [8] and Timoshenko et al. [9]. Warburton [10] analytically investigated the same problem studied by Fryba and Timoshenko, where his findings were confirmed by finite element analysis [11,12]. Using series solutions involving the Green function, Sadiku and Leipholz [13] compared the solutions for both the ''moving-mass moving-force'' problem and the equivalent ''moving-force'' problem and concluded that the inertia effect of the moving mass cannot be neglected in comparison with the gravitational effect even if the velocity of the moving mass is relatively small. However, the solutions presented were only for a particular combination of the mass and the vehicle speed.

Besides remaining a classical civil engineering problem, today the problem of moving loads on an elastic structure also arises in many modern machining operations such as ballistic machining and high-speed precision drilling. The interaction of the moving tool with the elastic structure creates forces dependant on both the tool suspension and the support beam characteristics. Katz et al. [14] examined the dynamic response of a constant-velocity moving load acting on a rotating shaft, on the basis of Euler–Bernoulli, Rayleigh and Timoshenko beam theories. Huang and Chen [15] reported the dynamic response of a rotating orthotropic beam subjected to a moving harmonic load, based on Euler–Bernoulli beam theory. All these approaches are based on the Euler–Bernoulli beam theory, and they refer to the interaction with a simply supported beam [16]. However, there are a large number of multi-span continuous bridges of large cross-section, and the effect of variation of the cross-sectional dimensions on the dynamic properties cannot be neglected. The effect of rotatory inertia and of shear deformation must be considered for those types of beam.

Esmailzadeh and Ghorashi [17] have tackled the problem of transverse vibration of simply supported beams traversed by uniform partially distributed moving masses. Furthermore, in a later study a comprehensive investigation into the dynamic response of a Timoshenko beam subjected to a partially distributed moving mass and the distribution of the shear force and bending moment along the beam has been carried out by Esmailzadeh and Ghorashi [18] and Wang [19]. Lee [20] utilized Hamilton's principle to solve the dynamic response of a beam with intermediate point constraints subjected to a moving load. Zheng et al. [21] studied the vibration

behavior of a multi-span continuous bridge modelled as a multi-span non-uniform continuous Euler–Bernoulli beam under a set of moving loads using different assumed mode shapes. Wu and Dai [22], Henchi and Fafard [23] used the same Euler–Bernoulli beam and the finite element transfer-matrix approach.

Due to new developments in rapid transport systems (fast cars and modern buses, high speed trains, trucks with multiple containers, etc.), it has become essential to study the behavior of bridges under moving loads at various speeds. Moreover, due to high-strength materials, bridge structures have become lighter and more flexible with longer spans, therefore requiring detailed consideration of high-frequency models and bridge–vehicle interaction analysis.

This paper further investigates the dynamics of vehicle–structure interaction of a bridge traversed by moving vehicles taking into account the passenger dynamics. The vehicle, including the driver and passenger, is modelled as a mobile half-car planar model, which is moving on a wide span uniform bridge modelled in the form of a simply supported Euler–Bernoulli beam. It is therefore expected that the consideration of the resilience and damping of the suspension system and the tire/road interactive forces would lead to a more realistic simulation of the earlier models. Simulation results are presented and a critical speed is found from which the maximum transversal dynamic deflection and the bending moment of the bridge attain their global maxima.

2. Bridges traversed by simple quarter-car model

A wide span bridge in the form of a simply supported uniform beam is traversed by a moving vehicle, in the form of a simple quarter-car (SQC) planar model, as shown in Fig. 1. The dynamic analysis of this problem is considerably more involved than for the one with a moving concentrated force of constant magnitude. The moving SQC model is considered as a dynamic system, with two degrees of freedom (d.o.f.), in which M_1 and M_2 are the unsprung mass and sprung mass of the moving vehicle respectively.

The tire is assumed to be in contact with the surface of the support beam at all times, and hence the moving tire will have the same vertical displacement as the bridge. The vertical displacements of the unsprung mass M_1 and that of the sprung mass M_2, with reference to their respective vertical equilibrium positions, are $y_1(t)$ and $y_2(t)$ respectively. The horizontal position of the center of the mass of the moving vehicle measured from the fixed reference point, such as the left end of the bridge, is denoted by x(t). The horizontal velocity and acceleration of the moving vehicle are v and a respectively.

The vertical interaction force $F(t)$ acting on the moving vehicle can therefore be written from the free-body diagrams of the moving vehicle as

$$\begin{aligned} F(t) &= C_1\left[\frac{\mathrm{d}y(t)}{\mathrm{d}t} - \frac{\mathrm{d}y_1(t)}{\mathrm{d}t}\right] + K_1[y(t) - y_1(t)] \\ &= M_1 g + M_1\frac{\mathrm{d}^2 y_1(t)}{\mathrm{d}t^2} + C_2\left[\frac{\mathrm{d}y_1(t)}{\mathrm{d}t} - \frac{\mathrm{d}y_2(t)}{\mathrm{d}t}\right] + K_2[y_1(t) - y_2(t)], \end{aligned} \tag{1}$$

in which g is the acceleration due to gravity. Notice that the first expression in Eq. (1) is obtained using force balance at the tire contact point with the road, while the second expression is rendered utilizing force balance at M_1.

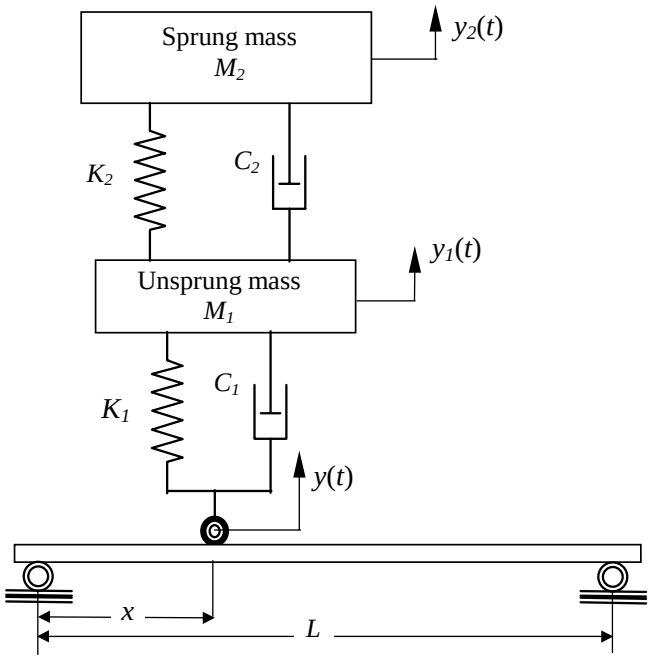

Fig. 1. Schematic of a suspension bridge traversed by a moving quarter-car model.

If there is no loss of contact between the tire and the upper surface of the bridge, the respective expressions for the vertical displacement, velocity and acceleration of the tire, moving along a vibrating curvilinear path, can be written as

$$y(t) = \{y(x,t) + r(x)\}_{x=x(t)}, \tag{2}$$

$$\dot{y}(t) = \frac{\mathrm{d}y(t)}{\mathrm{d}t} = \left\{\frac{\partial y}{\partial t} + v\frac{\partial y}{\partial x} + v\frac{\mathrm{d}r}{\mathrm{d}x}\right\}_{x=x(t)}, \tag{3}$$

and

$$\ddot{y}(t) = \frac{\mathrm{d}^2y(t)}{\mathrm{d}t^2} = \left\{\frac{\partial^2 y}{\partial t^2} + 2v\frac{\partial^2 y}{\partial x\partial t} + v^2\frac{\partial^2 y}{\partial x^2} + a\frac{\partial y}{\partial x} + v^2\frac{\mathrm{d}^2 r}{\mathrm{d}x^2} + a\frac{\mathrm{d}r}{\mathrm{d}x}\right\}_{x=x(t)}, \tag{4}$$

where $y(x,t)$ is the upward transversal dynamic deflection of the bridge structure and $r(x)$ is the surface roughness of the bridge which refers to the road waviness and is represented as the vertically upward departure from the mean horizontal profile.

The first term on the right-hand of Eq. (4) is the support beam acceleration at the point of contact with the moving vehicle and the second term denotes the well-known Coriolis acceleration, since the vehicle is moving along a vibrating curvilinear path (i.e., the support beam). The third term on the right-hand of Eq. (4) is the centripetal acceleration of the moving vehicle and the fourth term indicates the acceleration component in the vertical direction when the moving vehicle speed is not assumed as constant. The fifth term on the right-hand of Eq. (4) represents the centripetal acceleration of the moving vehicle on the road waviness of the upper

surface of the bridge, while the last term is the acceleration component in the vertical direction when the speed of the moving vehicle travels on the road surface of the bridge is not constant.

From Eqs. (1)–(4), it can be seen that the interaction force, $F(t)$, between the moving vehicle and the bridge depends on the velocity and acceleration of the vehicle, the flexibility of the bridge structure, and the road waviness of the upper surface of the bridge. The interaction force does indeed vary with time and it can be taken as an indicator of separation. When this force becomes zero, it denotes the onset of separation, and it should remain zero until the moving vehicle re-establishes contact with the bridge surface. This interaction will be considered when studying a more realistic model for the vehicle as described next.

3. Half-car planar model moving on a beam

This section considers the dynamical analysis and the mathematical model developed for the passenger–vehicle–bridge interaction. For this study, only linear models are assumed to represent both the vehicle suspension systems and the bridge dynamics. However, further work is in progress for the cases that involve the non-linear models of the bridge and the vehicle suspension system.

3.1. System formulation and assumptions

The bridge characteristic, modelled in its simple form, is described by the Euler–Bernoulli beam theory. Although the bridge model may include additional effects of the Timoshenko beam theory or the unconventional boundary conditions, these are not included at this phase of study, and instead attention is focused on the passenger–vehicle–bridge interaction problem.

It is assumed that the vehicle advances along the bridge with the velocity $\dot{u}(t)$, where $u(t)$ is the position of the center of gravity (c.g.) of the vehicle body measured from the left-end support of the bridge, as shown in Fig. 2. Moreover, at $t = 0$ the front tire of the vehicle initially enters the bridge, from the left-end support, and both the front and rear tires remain in contact with the bridge surface at all times.

The vehicle is assumed as a half-car planar model with six d.o.f, which consists of a body (sprung mass), two axles (unsprung masses), driver and a passenger. The body is considered to have the vertical motion (bounce) and the angular motion (pitch), with every axle having its own bounce. The driver and the passenger are constrained to have only their own vertical oscillations. The compliances of the suspension system, the tires, and the passenger seats are modelled by the combination of linear springs and viscous dampers connected in parallel arrangements.

The bridge is modelled as a uniform simply supported beam and initially is considered free of any load or deflection, and hence is horizontal at the equilibrium position under its own weight (unloaded). The steady state displacements of the vehicle are also measured from their static equilibrium positions obtained just before the vehicle enters the bridge. Therefore, the gravitational effect of the vehicle weight forms an additional part of the variable moving loads acting on the bridge.

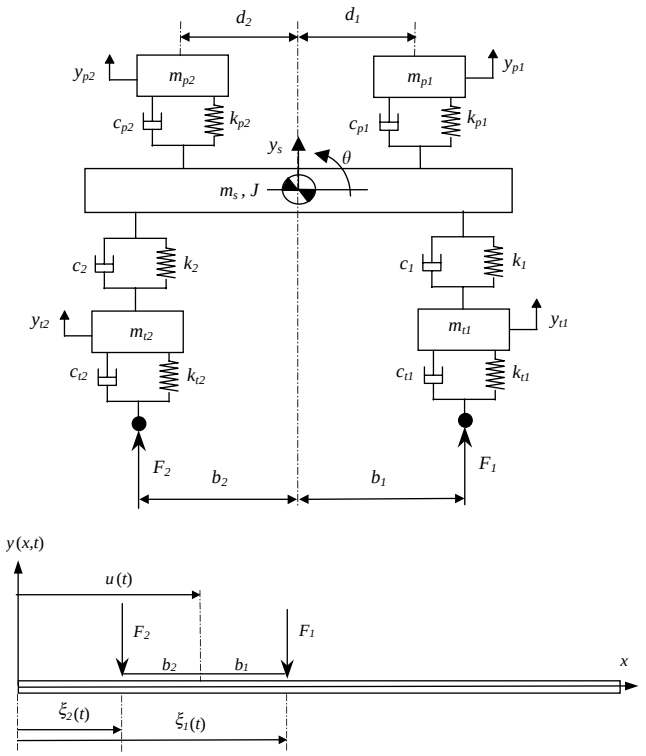

Fig. 2. Suspension system of a 6-d.o.f. half-car model moving on a bridge.

3.2. Governing equations of motion

In order to generate the governing equations of motion for the passenger–vehicle–bridge interaction model, the energy method is applied. To characterize the transverse elastic deformation of the bridge, one could associate the displacement $y(x,t)$ to every point on the undeformed neutral axis of the bridge (beam), where x is the reference variable along the length of the beam measured from the left-end support, and t is the elapsed time.

In the derivation that follows, the shorthand notations dot "$\cdot$" and prime "$'$" represent the partial derivative of the variables with respect to the time t and the position x respectively.

Under the assumptions put forward in the preceding subsection, the kinetic energy of the system may now be expressed as

$$T = \frac{1}{2}\Big\{ \int_0^L \rho[\dot{y}^2(x,t)]\,\mathrm{d}x + m_s\dot{y}_s^2(t) + J\dot{\theta}^2(t) + m_{p1}\dot{y}_{p1}^2(t) + m_{p2}\dot{y}_{p2}^2(t) + m_{t1}\dot{y}_{t1}^2(t) + m_{t2}\dot{y}_{t2}^2(t)\Big\}, \tag{5}$$

where ρ is the mass per unit length of the uniform beam, and the other parameters involved are defined in Fig. 2.

The potential energy of this system, using linear strains assumption, can be written as

$$\begin{aligned} U = \frac{1}{2}\Big\{ & \int_0^L EI[y''^2(x,t)]\,\mathrm{d}x + k_{p1}[y_s(t) + d_1\theta(t) - y_{p1}(t)]^2 \\ & + k_{p2}[y_s(t) - d_2\theta(t) - y_{p2}(t)]^2 + k_1[y_s(t) + b_1\theta(t) - y_{t1}(t)]^2 \\ & + k_2[y_s(t) - b_2\theta(t) - y_{t2}(t)]^2 + k_{t1}[y_{t1}(t) - y(\xi_1(t),t)]^2 H(x - \xi_1(t)) \\ & + k_{t2}[y_{t2}(t) - y(\xi_2(t),t)]^2 H(x - \xi_2(t))\Big\}, \end{aligned} \tag{6}$$

where EI is the flexural rigidity of the beam, and $H(x)$ is the Heaviside function. The locations of the contact points of the front and rear tires with the bridge surface are given by the expressions

$$\xi_1(t) = u(t) + b_1, \qquad \xi_2(t) = u(t) - b_2. \tag{7}$$

It should be noted that the axial strain energy, which contains only the terms of higher order than quadratic in the elastic variable y, has not been included in the potential energy U for the consistency of the formulation.

The governing equations of motion may now be derived by applying Hamilton's principle. However, to facilitate the analysis, we resort to an assumed mode expansion and the Lagrange's equations. Specifically, the elastic variable y could be written as the finite sum of the well-known Galerkin approximation

$$y(x,t) = \sum_{i=1}^{n} \phi_i(x) q_i(t), \tag{8}$$

where $q_i(t)$ are the generalized co-ordinates for the elastic deflection of the beam element, and $\phi_i(x)$ are the transverse eigenfunctions (i.e., modal shapes) of a beam with the general form of the conventional boundary conditions.

The orthogonality conditions between these mode shapes can also be derived as [24,25]

$$\int_0^L \rho\phi_i(x)\phi_j(x)\,\mathrm{d}x = N_i\delta_{ij} \qquad \int_0^L EI\phi_i''(x)\phi_j''(x)\,\mathrm{d}x = S_i\delta_{ij}, \tag{9}$$

where δ_{ij} is the Kronecker delta for $i,j = 1,2,\ldots,n$, and N_i and S_i are defined by setting $i = j$ in Eq. (9).

The effect of the vehicle weight acting on the bridge and the dissipating damping forces in both the vehicle suspensions and the bridge structure are considered as non-conservative forces in Lagrange's formulation. The time-varying gravitational force, in terms of the Heaviside function, is expressed as

$$\begin{aligned} f_g(x,t) &= -\left(m_{t1} + m_s\frac{b_2}{b_1+b_2} + m_{p1}\frac{b_2+d_1}{b_1+b_2} + m_{p2}\frac{b_2-d_2}{b_1+b_2}\right) gH(x-\xi_1(t)) \\ &\quad - \left(m_{t2} + m_s\frac{b_1}{b_1+b_2} + m_{p1}\frac{b_1-d_1}{b_1+b_2} + m_{p2}\frac{b_1+d_2}{b_1+b_2}\right) gH(x-\xi_2(t)) \\ &= -(f_{g1}H(x-\xi_1(t)) + f_{g2}H(x-\xi_2(t))). \end{aligned} \tag{10}$$

The Rayleigh's dissipation function can be written as

$$\begin{aligned} R = &\tfrac{1}{2}\{c\dot{y}^2(x,t) + c_{p1}[\dot{y}_s(t) + d_1\dot{\theta}(t) - \dot{y}_{p1}(t)]^2 \\ &+ c_{p2}[\dot{y}_s(t) - d_2\dot{\theta}(t) - \dot{y}_{p2}(t)]^2 + c_1[\dot{y}_s(t) + b_1\dot{\theta}(t) - \dot{y}_{t1}(t)]^2 \\ &+ c_2[\dot{y}_s(t) - b_2\dot{\theta}(t) - \dot{y}_{t2}(t)]^2 + c_{t1}[\dot{y}_{t1}(t) - \dot{y}(\xi_1(t),t)]^2 H(x-\xi_1(t)) \\ &+ c_{t2}[\dot{y}_{t2}(t) - \dot{y}(\xi_2(t),t)]^2 H(x-\xi_2(t)), \end{aligned} \tag{11}$$

where c is the equivalent linear coefficient of the damping of the bridge.

The Lagrange's equations for the six variables involved can be expressed as

$$\begin{aligned} &\frac{\mathrm{d}}{\mathrm{d}t}\left(\frac{\partial T}{\partial \dot{p}_k(t)}\right) - \frac{\partial T}{\partial p_k(t)} + \frac{\partial U}{\partial p_i(t)} + \frac{\partial R}{\partial \dot{p}_k(t)} = 0, \quad k = 1,2,\ldots,6, \\ &\frac{\mathrm{d}}{\mathrm{d}t}\left(\frac{\partial T}{\partial \dot{q}_i(t)}\right) - \frac{\partial T}{\partial q_i(t)} + \frac{\partial U}{\partial q_i(t)} + \frac{\partial R}{\partial \dot{q}_i(t)} = Q_i, \quad i = 1,2,\ldots,n, \end{aligned} \tag{12}$$

where the state variables vector for the passenger-vehicle is

$$\mathbf{p}(t) = \{\, y_s(t) \quad \theta(t) \quad y_{p1}(t) \quad y_{p2}(t) \quad y_{t1}(t) \quad y_{t2}(t) \,\}^{\mathrm{T}}.$$

Moreover, the expression for the generalized force Q_i could be written as

$$Q_i = \int_0^L \phi_i(x) f_g(x,t)\,\mathrm{d}x, \quad i = 1,2,\ldots,n. \tag{13}$$

By taking into account the orthogonality conditions given by Eq. (9) and the Galerkin approximation of Eq. (8), the governing equations of motion can now be derived. The passenger–vehicle model is governed by six linear second order differential equations of motion, which can be derived in the general form.

The equation of the vertical motion (bounce) for the sprung mass (body) is

$$\begin{aligned} &m_s\ddot{y}_s(t) + c_1[\dot{y}_s(t) + b_1\dot{\theta}(t) - \dot{y}_{t1}(t)] + c_{p1}[\dot{y}_s(t) + d_1\dot{\theta}(t) - \dot{y}_{p1}(t)] \\ &\quad + c_2[\dot{y}_s(t) - b_2\dot{\theta}(t) - \dot{y}_{t2}(t)] + c_{p2}[\dot{y}_s(t) - d_2\dot{\theta}(t) - \dot{y}_{p2}(t)] \\ &\quad + k_1[y_s(t) + b_1\theta(t) - y_{t1}(t)] + k_{p1}[y_s(t) + d_1\theta(t) - y_{p1}(t)] \\ &\quad + k_2[y_s(t) - b_2\theta(t) - y_{t2}(t)] + k_{p2}[y_s(t) - d_2\theta(t) - y_{p2}(t)] = 0, \end{aligned} \tag{14}$$

and the equation of the angular motion (pitch) of the sprung mass has the form of

$$\begin{aligned} &J\ddot{\theta}(t) + c_1b_1[\dot{y}_s(t) + b_1\dot{\theta}(t) - \dot{y}_{t1}(t)] + c_{p1}d_1[\dot{y}_s(t) + d_1\dot{\theta}(t) - \dot{y}_{p1}(t)] \\ &\quad - c_2b_2[\dot{y}_s(t) - b_2\dot{\theta}(t) - \dot{y}_{t2}(t)] - c_{p2}d_2[\dot{y}_s(t) - d_2\dot{\theta}(t) - \dot{y}_{p2}(t)] \\ &\quad + k_1b_1[y_s(t) + b_1\theta(t) - y_{t1}(t)] + k_{p1}d_1[y_s(t) + d_1\theta(t) - y_{p1}(t)] \\ &\quad - k_2b_2[y_s(t) - b_2\theta(t) - y_{t2}(t)] - k_{p2}d_2[y_s(t) - d_2\theta(t) - y_{p2}(t)] = 0. \end{aligned} \tag{15}$$

The equation of the vertical motion (bounce) of the driver is

$$\begin{aligned} &m_{p1}\ddot{y}_{p1}(t) + c_{p1}[\dot{y}_{p1}(t) - \dot{y}_s(t) - d_1\dot{\theta}(t)] \\ &\quad + k_{p1}[y_{p1}(t) - y_s(t) - d_1\theta(t)] = 0, \end{aligned} \tag{16}$$

while the vertical motion (bounce) of the passenger is governed by

$$m_{p2}\ddot{y}_{p2}(t) + c_{p2}[\dot{y}_{p2}(t) - \dot{y}_s(t) + d_2\dot{\theta}(t)] + k_{p2}[y_{p2}(t) - y_s(t) + d_2\theta(t)] = 0. \tag{17}$$

The equation of the vertical motion (bounce) for the front axle is

$$m_{t1}\ddot{y}_{t1}(t) + c_1[\dot{y}_{t1}(t) - \dot{y}_s(t) - b_1\dot{\theta}(t)] + c_{t1}[\dot{y}_{t1}(t) - \dot{y}(\xi_1(t), t)D_1] + k_1[y_{t1}(t) - y_s(t) - b_1\theta(t)] + k_{t1}[y_{t1}(t) - y(\xi_1(t), t)D_1] = 0 \tag{18}$$

and the vertical motion (bounce) of the rear axle is governed by

$$m_{t2}\ddot{y}_{t2}(t) + c_2[\dot{y}_{t2}(t) - \dot{y}_s(t) + b_2\dot{\theta}(t)] + c_{t2}[\dot{y}_{t2}(t) - \dot{y}(\xi_2(t), t)D_2] + k_2[y_{t2}(t) - y_s(t) + b_2\theta(t)] + k_{t2}[y_{t2}(t) - y(\xi_2(t), t)D_2] = 0. \tag{19}$$

The dynamics of the bridge is described by n second order differential equations given by

$$N_i\ddot{q}_i(t) + S_iq_i(t) + D_1\phi_i(\xi_1(t))\{f_{g1} + c_{t1}[\dot{y}(\xi_1(t), t)D_1 - \dot{y}_{t1}(t)] + k_{t1}[y(\xi_1(t), t)D_1 - y_{t1}(t)]\} + D_2\phi_i(\xi_2(t))\{f_{g2} + c_{t2}[\dot{y}(\xi_2(t), t)D_2 - \dot{y}_{t2}(t)] + k_{t2}[y(\xi_2(t), t)D_2 - y_{t2}(t)]\} = 0, \quad i = 1, 2, \ldots, n, \tag{20}$$

where coefficients D_1 and D_2 depend on the interval of the motion defined by the following four stages

$$\begin{cases} 0 \leqslant t < t_1, & D_1 = 1, D_2 = 0, \\ t_1 \leqslant t < t_2, & D_1 = 1, D_2 = 1, \\ t_2 \leqslant t < t_3, & D_1 = 0, D_2 = 1, \\ t_3 \leqslant t, & D_1 = 0, D_2 = 0, \end{cases} \tag{21}$$

in which the parameters t_1, t_2, and t_3 are the respective times when the second tire enters the bridge, the first tire leaves the bridge, and the second tire leaves the bridge.

Eqs. (14)–(20) form a system of $(n + 6)$ second order coupled differential equations with time-varying coefficients. Obviously, the two coefficients D_1 and D_2 and the eigen-functions $\phi_i(\xi_1(t))$ and $\phi_i(\xi_2(t))$ represent these time-varying coefficients in the governing equations of motion.

The above equations could simply be represented in the state-space form

$$\dot{\mathbf{x}}(t) = \mathbf{A}(t)\mathbf{x}(t) + \mathbf{f}(t), \tag{22}$$

where

$$\mathbf{x}(t) = \begin{Bmatrix} \mathbf{x}_1(t) \\ \dot{\mathbf{x}}_1(t) \end{Bmatrix}, \qquad \mathbf{x}_1(t) = \{\mathbf{p}^{\mathrm{T}}(t) | q_{1(t)} \cdots q_n(t)\}^{\mathrm{T}},$$

$$\mathbf{A} = \left[\begin{array}{ccc|ccc} & \mathbf{0}_{(n+6)\times(n+6)} & & & \mathbf{I}_{(n+6)\times(n+6)} & \\ \hline \boldsymbol{\Gamma}_{6\times6} & & \mathbf{0}_{6\times n} & \boldsymbol{\Lambda}_{6\times6} & & \mathbf{0}_{6\times n} \\ \mathbf{0}_{n\times4} & \mathbf{V}_{n\times2} & \mathbf{S}_{n\times n} & \mathbf{0}_{n\times4} & \boldsymbol{\Omega}_{n\times2} & \boldsymbol{\Psi}_{n\times n} \end{array}\right]_{2(n+6)\times2(n+6)}, \tag{23}$$

$$\mathbf{f}(t) = \begin{bmatrix} \mathbf{0}_{(n+12)\times 1} \\ \mathbf{P}_{n\times 1} \end{bmatrix}_{2(n+6)\times 1},$$

in which $\mathbf{\Gamma}_{6\times 6}$ is a constant matrix consisting of vehicle spring constants, $\mathbf{\Lambda}_{6\times 6}$ is a constant matrix representing the vehicle damper constants, and the rest of non-zero and non-unity matrices are time-varying as defined by

$$\mathbf{V} = \begin{bmatrix} k_{t1}D_1\phi_1(\xi_1(t)) & k_{t2}D_2\phi_1(\xi_2(t)) \\ \vdots & \vdots \\ k_{t1}D_1\phi_n(\xi_1(t)) & k_{t2}D_2\phi_n(\xi_2(t)) \end{bmatrix}_{n\times 2}, \qquad \mathbf{\Omega} = \begin{bmatrix} c_{t1}D_1\phi_1(\xi_1(t)) & c_{t2}D_2\phi_1(\xi_2(t)) \\ \vdots & \vdots \\ c_{t1}D_1\phi_n(\xi_1(t)) & c_{t2}D_2\phi_n(\xi_2(t)) \end{bmatrix}_{n\times 2},$$

$$\mathbf{S} = \begin{bmatrix} (-k_{t1}D_1^2\phi_1^2(\xi_1(t)) - k_{t2}D_2^2\phi_1^2(\xi_2(t)))/N_1 & \cdots & (-k_{t1}D_1^2\phi_n^2(\xi_1(t)) - k_{t2}D_2^2\phi_n^2(\xi_2(t)))/N_1 \\ \vdots & & \vdots \\ (-k_{t1}D_1^2\phi_1^2(\xi_1(t)) - k_{t2}D_2^2\phi_1^2(\xi_2(t)))/N_n & \cdots & (-k_{t1}D_1^2\phi_n^2(\xi_1(t)) - k_{t2}D_2^2\phi_n^2(\xi_2(t)))/N_n \end{bmatrix}_{n\times n},$$

$$\mathbf{\Psi} = \begin{bmatrix} (-c_{t1}D_1^2\phi_1^2(\xi_1(t)) - c_{t2}D_2^2\phi_1^2(\xi_2(t)))/N_1 & \cdots & (-c_{t1}D_1^2\phi_n^2(\xi_1(t)) - c_{t2}D_2^2\phi_n^2(\xi_2(t)))/N_1 \\ \vdots & & \vdots \\ (-c_{t1}D_1^2\phi_1^2(\xi_1(t)) - c_{t2}D_2^2\phi_1^2(\xi_2(t)))/N_n & \cdots & (-c_{t1}D_1^2\phi_n^2(\xi_1(t)) - c_{t2}D_2^2\phi_n^2(\xi_2(t)))/N_n \end{bmatrix}_{n\times n},$$

$$\mathbf{P} = \begin{bmatrix} -D_1\phi_1(\xi_1(t)f_{g1} - D_2\phi_1(\xi_2(t)f_{g2} \\ \vdots \\ -D_1\phi_n(\xi_1(t)f_{g1} - D_2\phi_n(\xi_2(t)f_{g2} \end{bmatrix}_{n\times 1}.$$

The eigen functions $\phi_i(x)$, based on the Euler–Bernoulli beam theory, are utilized in the solution. For the numerical example given here, the normalized eigenfunctions of a simply supported beam are given by

$$\phi_i(x) = \sqrt{\frac{2}{L}}\sin\left(\frac{\mathrm{i}\pi x}{L}\right), \quad i = 1, 2, \ldots, n. \tag{24}$$

4. Vehicle critical speed

When the vehicle advances along the bridge at a specified constant speed, $V = \dot{u}(t) = \text{constant}$, the resulting variable moving force may almost excite one of the fundamental modes of the vibration of the bridge. The amplitude of the transversal vibration of the bridge and the bending moment induced in the beam structure, while the vehicle travels on the bridge, would attain their maximum value at the certain position and instant of time. The location of these maximum transversal deflections and the bending moment of the beam, their amplitudes, and the corresponding vehicle speed are important factors for the bridge designers as well as the traffic regulation authorities. The critical speed that can be properly posted, for instance at the bridge entrance, would certainly avoid the large transversal dynamic deflection and the bending moment induced in the bridge.

The maximum amplitude of the transversal deflection of the bridge, for a specified speed of the vehicle, can be obtained from

$$y_{max} = \max\{|y(x,t)|, 0 \leqslant x \leqslant L, 0 \leqslant t \leqslant t_3\}. \tag{25}$$

Moreover, the maximum value of the bending moment induced in the bridge is given by

$$M_{max} = \max\{|M_b(x,t)|, 0 \leqslant x \leqslant L, 0 \leqslant t \leqslant t_3\}, \tag{26}$$

where the bending moment M_b for small values of displacements and slopes is related to the deflection $y(x,t)$ by the equation

$$M_b(x,t) = -EIy''(x,t).$$

To find the critical speed of the vehicle, for attaining the maximum value of the bending moment and the transversal dynamic deflection, a search must be carried out for different values of the vehicle speed. For each value of the constant vehicle speed, these maxima (y_{max} and M_{max}) can be evaluated and their variations versus vehicle speed will render the required critical speeds, from which the values of y_{max} and M_{max} attain their global maxima. A detailed and systematic procedure to determine these maxima is described in the following numerical section.

5. Numerical simulations and results

The analysis of a case study, in which a vehicle travels at a constant speed on a bridge, is presented here. The 6-d.o.f. passenger–vehicle planar model, shown in Fig. 2, is considered here to be in 2-D plane. The numerical values of the parameters, arbitrary chosen for the computer simulation analysis, are as follows:

Bridge:

$$L = 100\,\text{m}, E = 207\,\text{GPa}, I = 0.174\ \text{m}^4, \rho = 20\,000\ \ \text{kg/m}, c = 1750\,\text{N s/m}.$$

Vehicle:

$$m_s = 1794.4\,\text{kg}, m_{t1} = 87.15\,\text{kg}, m_{t2} = 140.4\,\text{kg}, m_{p1} = m_{p2} = 75\,\text{kg},$$

$$J = 3443.05\,\text{kg m}^2, b_1 = 1.271, b_2 = 1.716, d_1 = 0.481, d_2 = 1.313\,\text{m},$$

$$k_1 = 66824.4, k_2 = 18615.0, k_{t1} = k_{t2} = 101115.0, k_{p1} = k_{p2} = 14000.0\,\text{N/m},$$

$$c_1 = 1190, c_2 = 1000, c_{t1} = c_{t2} = 14.6, c_{p1} = 50.2, c_{p2} = 62.1\,\text{N s/m}.$$

Initially, the effects of the number of modes (i.e., n) on the transversal deformation of the beam were studied, and consequently, a minimum number of four natural modes were chosen. This critical selection is made based on the evolution of the deflection of the beam at the mid-span, as the number of modes taken in the model increased from three. For numerical simulations, the system of differential equations (22) was numerically solved using MATLAB® [26] and MAPLE® [27] software packages.

The time history diagram for the transversal dynamic deflection of the mid-span of the bridge for different values of the vehicle speed is shown in Fig. 3, while the transient response for the bounce motion of the vehicle body is illustrated in Fig. 4. The variations of the bounce motion of

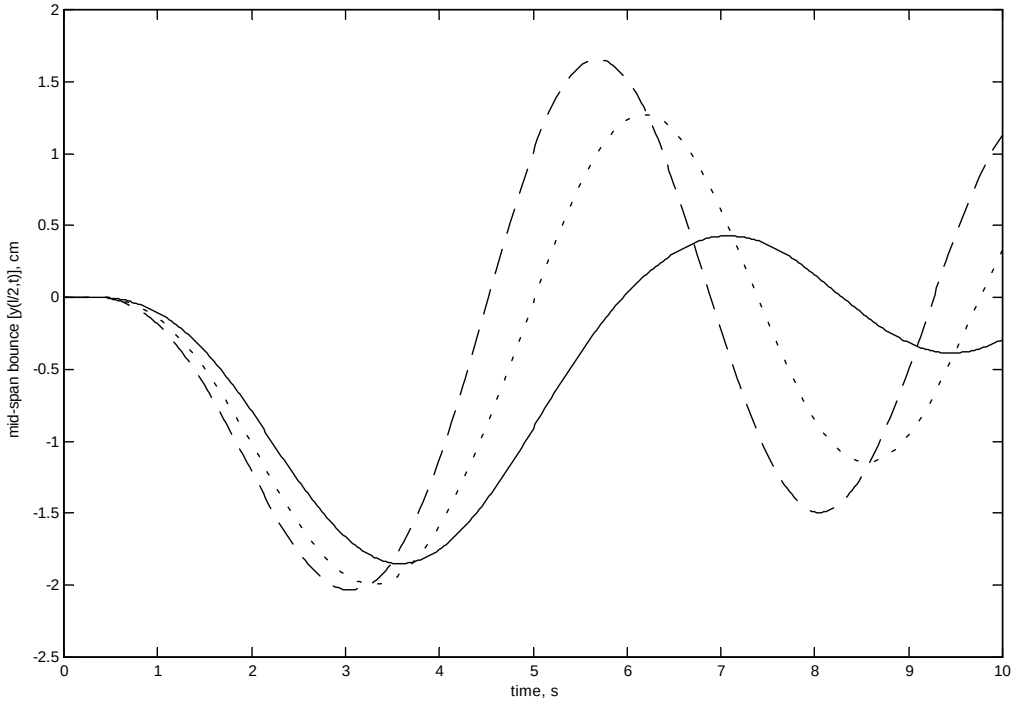

Fig. 3. Time history of mid-span deflection of the beam for $V = 56$ (—), $V = 72$ (. . . .), and $V = 88$ km/h (- - -).

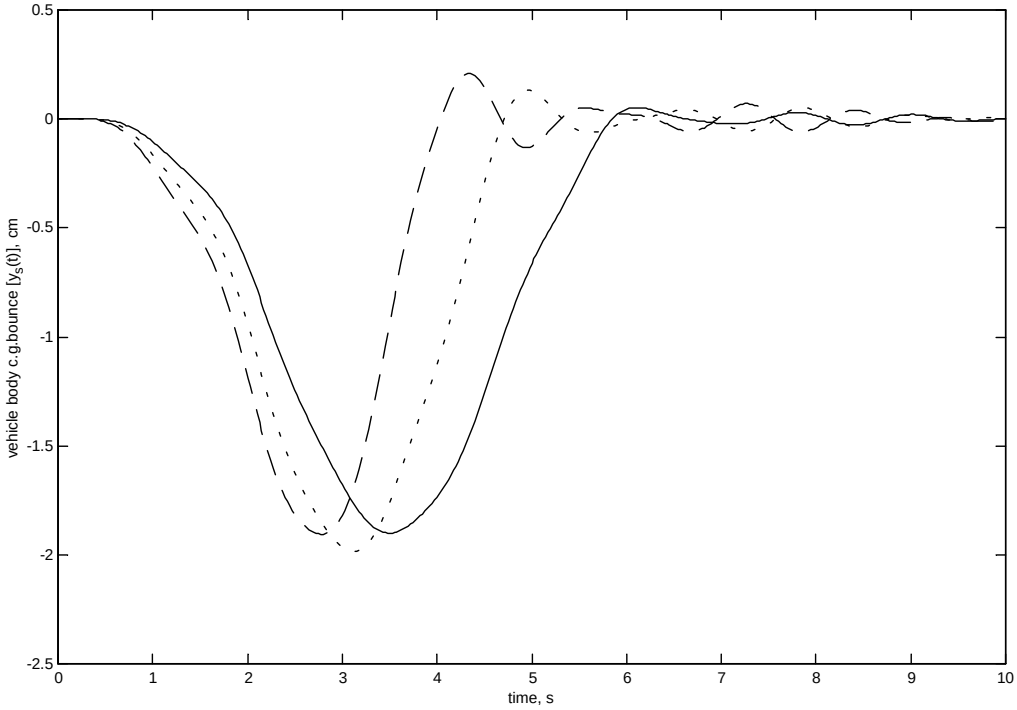

Fig. 4. Time history of vehicle body bounce for $V = 56$ (—), $V = 72$ (. . . .), and $V = 88$ km/h (- - -).

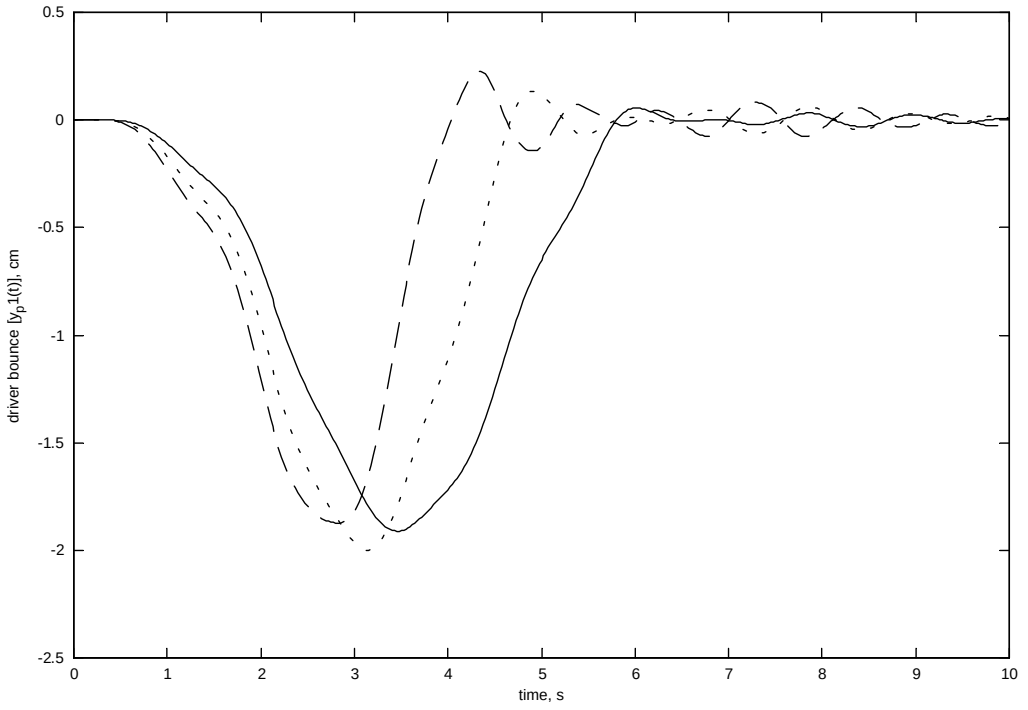

Fig. 5. Time history of driver bounce for $V = 56$ (—), $V = 72$ (. . . .), and $V = 88$ km/h (- - -).

the driver and the passenger as a function of time and vehicle speed are shown in Figs. 5 and 6, respectively. It is clear that as the speed of the vehicle changes, it affects the induced vibration generated at the driver and the passenger subsections. Moreover, the time history diagrams of the front and rear tire bounce for different values of the vehicle speed are presented in Figs. 7 and 8, respectively. From the simulation results obtained, one could see that as the speed of the vehicle increases, greater values of the transversal dynamic deflections for the bridge would be obtained. The total duration time of the presence of the vehicle on the bridge, for the vehicle speeds of 56, 72, and 88 km/h, are 6.6, 5.1, and 4.2 s, respectively.

The same analysis can be performed utilizing the SQC model, where the half-car planar model of Fig. 2 is reduced to the one depicted in Fig. 1. For the sake of comparison, we select the bridge parameters the same as given above with the equivalent values for the SQC model as (see Fig. 1):

$$M_2 = m_s + m_{p1} + m_{p2}, \quad M_1 = m_{t1} + m_{t2}, \quad f_g = -(M_1 + M_2)gH(x - \xi(t)),$$
$$K_2 = k_1 + k_2, \quad K_1 = k_{t1} + k_{t2}, \quad C_2 = c_1 + c_2, \quad C_1 = c_{t1} + c_{t2}.$$

When simulation results for the beam mid-span deflection and vehicle body bounce are compared for SQC and half-car planar models, the plots depicted in Figs. 9 and 10 are obtained. Notice that this comparison for other variables such as the front and rear tire deflections is not suitable as they do not exist in the SQC model. It is clear that the use of the SQC model does not provide adequate information for both vehicle dynamics and bridge characteristics, when compared with the half-car model (see Figs. 9 and 10).

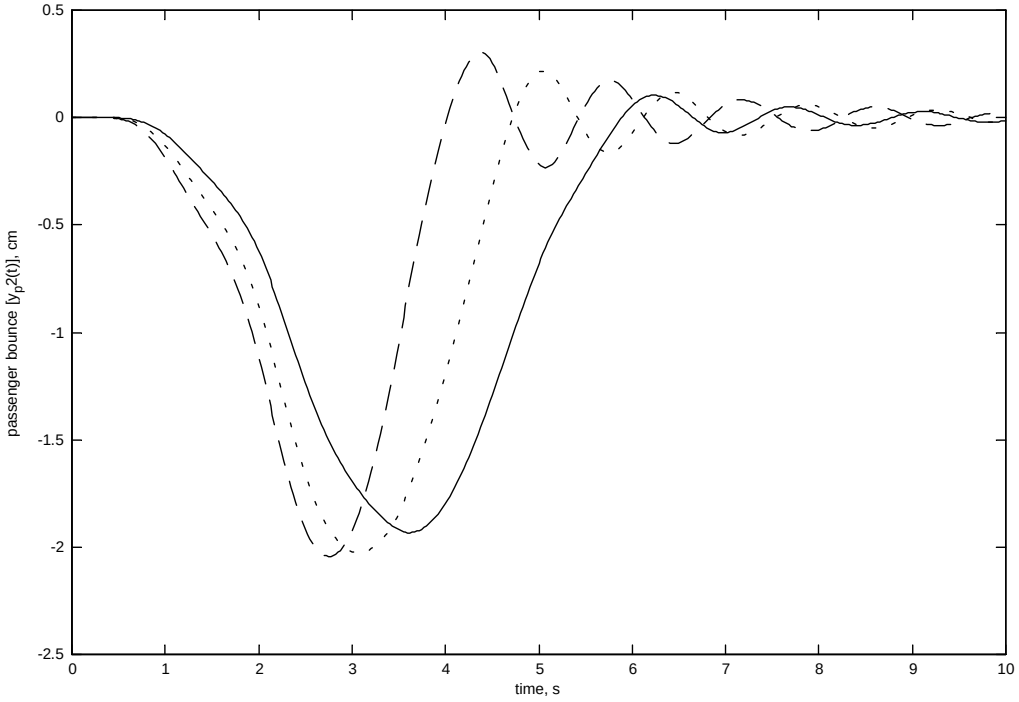

Fig. 6. Time history of passenger bounce for $V = 56$ (—), $V = 72$ (. . . .), and $V = 88$ km/h (- - -).

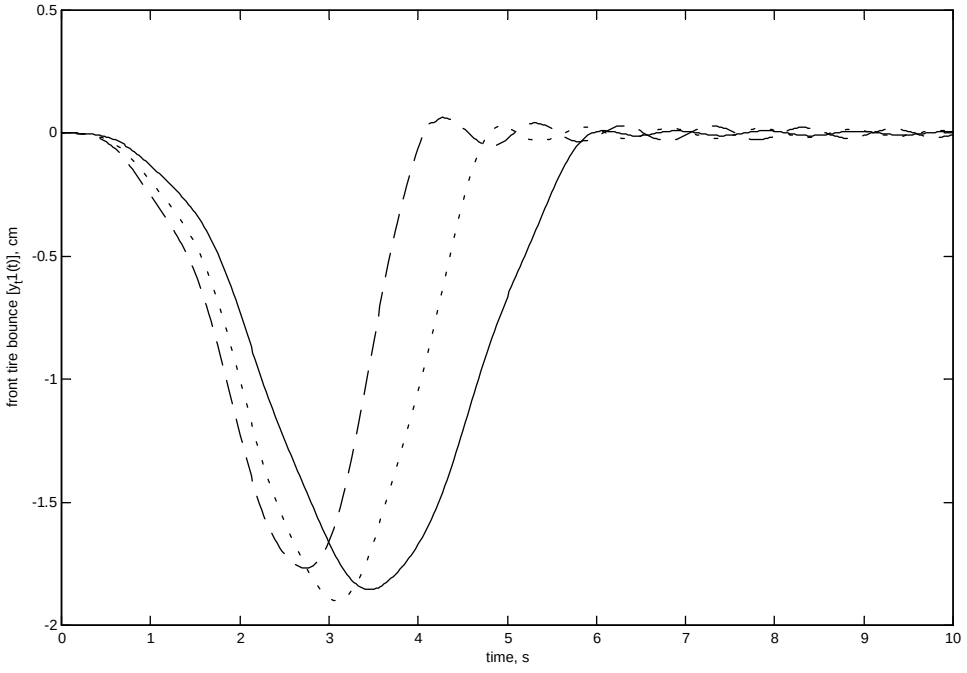

Fig. 7. Time history of front tire bounce for $V = 56$ (—), $V = 72$ (. . . .), and $V = 88$ km/h (- - -).

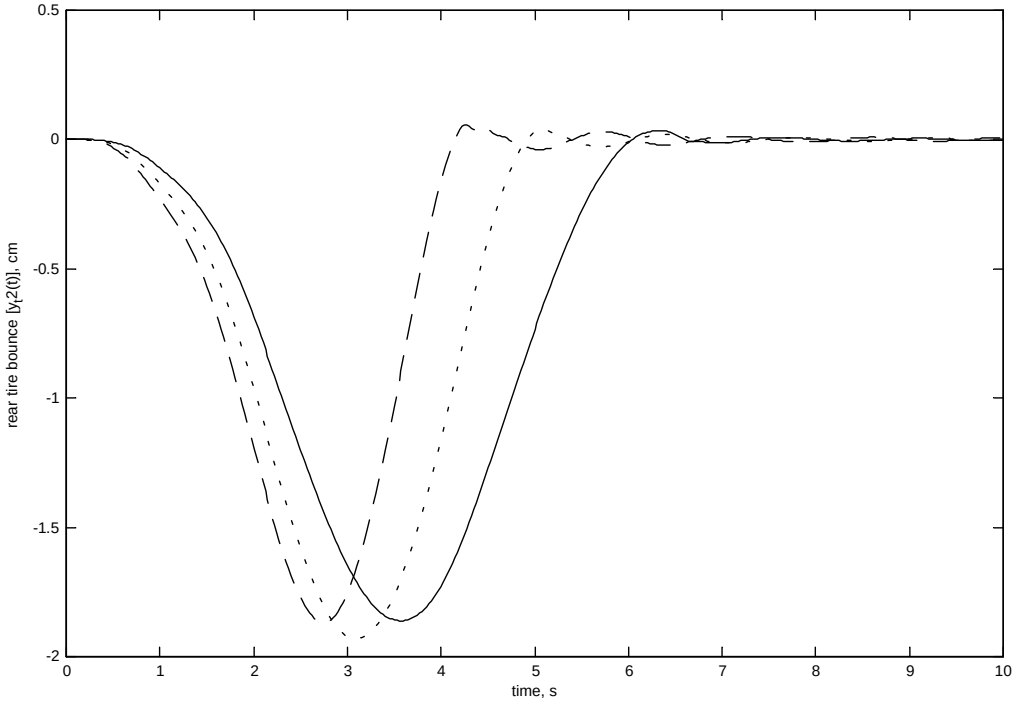

Fig. 8. Time history of rear tire bounce for $V = 56$ (—), $V = 72$ (. . . .), and $V = 88$ km/h (- - -).

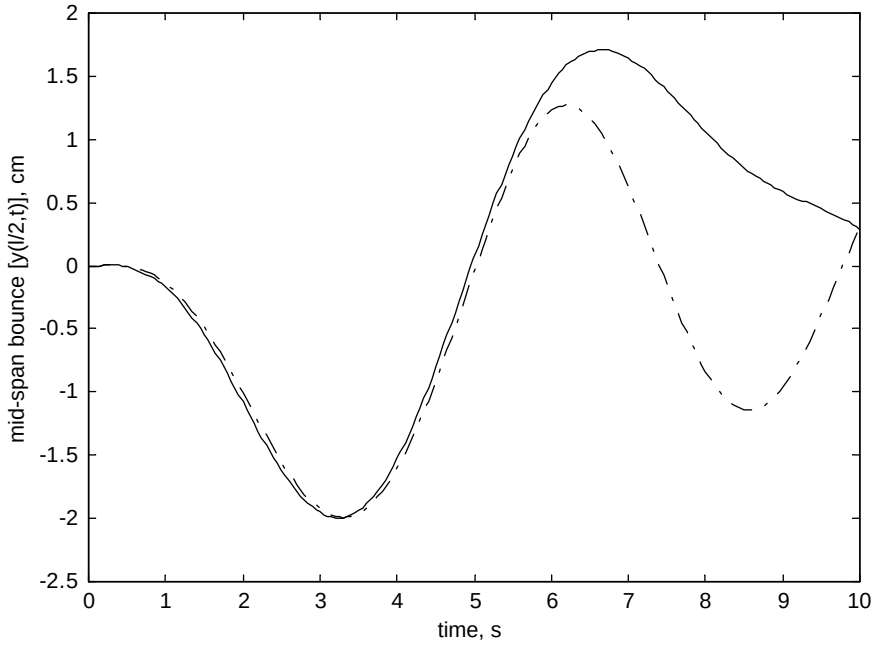

Fig. 9. Comparison between beam mid-span deflection for SQC (—) and half-car (- - -) models ($V = 72$ km/h).

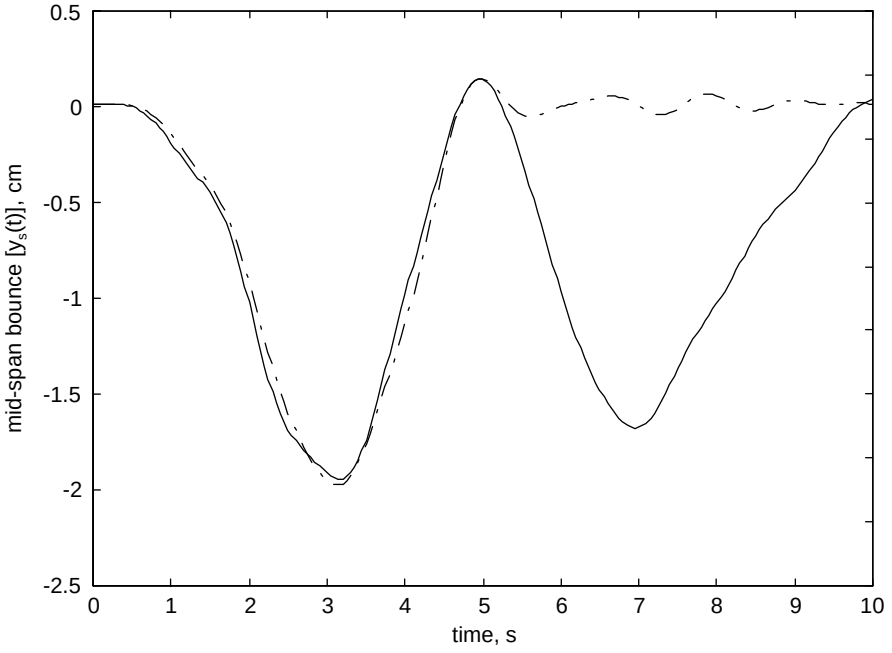

Fig. 10. Comparison between vehicle body bounce for SQC (—) and half-car (- - -) models ($V = 72$ km/h).

The values of the maximum transversal dynamic deflection and the generated bending moment with their exact locations along the bridge are very important when designing bridges traversed by moving vehicles. The time variations of the maximum dynamic deflection and the bending moment induced in the bridge structure are illustrated in Figs. 11 and 12 respectively. It can be seen that the peak values occur at different locations for the transversal dynamics deflection (Fig. 11(b)) and the bending moment (Fig. 12(b)), which are compared with those in Fig. 13 for the vehicle speed of 56 km/h.

One may note that these diagrams are not for the time history at a certain point of the bridge, though they represent the maximum values of the transversal dynamic deflection and the bending moment induced at different points along the bridge at each instant of time. Since the location of the maximum dynamic deflections occurs almost at mid-span (or at $\pm 3\%$ vicinity of mid-span) Fig. 11(a) seems very similar to Fig. 3, though they represent two different characteristics as explained before.

In order to determine the critical speed of the vehicle, mentioned in Section 4, the following steps are taken:

(1) For a constant vehicle speed, initially the maximum transversal dynamic deflections at each point along the bridge and over the time interval $t \in [0, t_3]$ are determined. This vector is denoted by $\mathbf{y}^t_{max}$.
(2) The maximum transversal dynamic deflection at each instant of time and over the entire length of the bridge $x \in [0, L]$ is then obtained. The resulting vector is called $\mathbf{y}^x_{max}$.
(3) The maximum value of $\mathbf{y}^t_{max}$, found over different points along the length of the bridge, and its corresponding location point are now obtained. They are denoted as $y_{max\,max}$ and $x_{max:max}$,

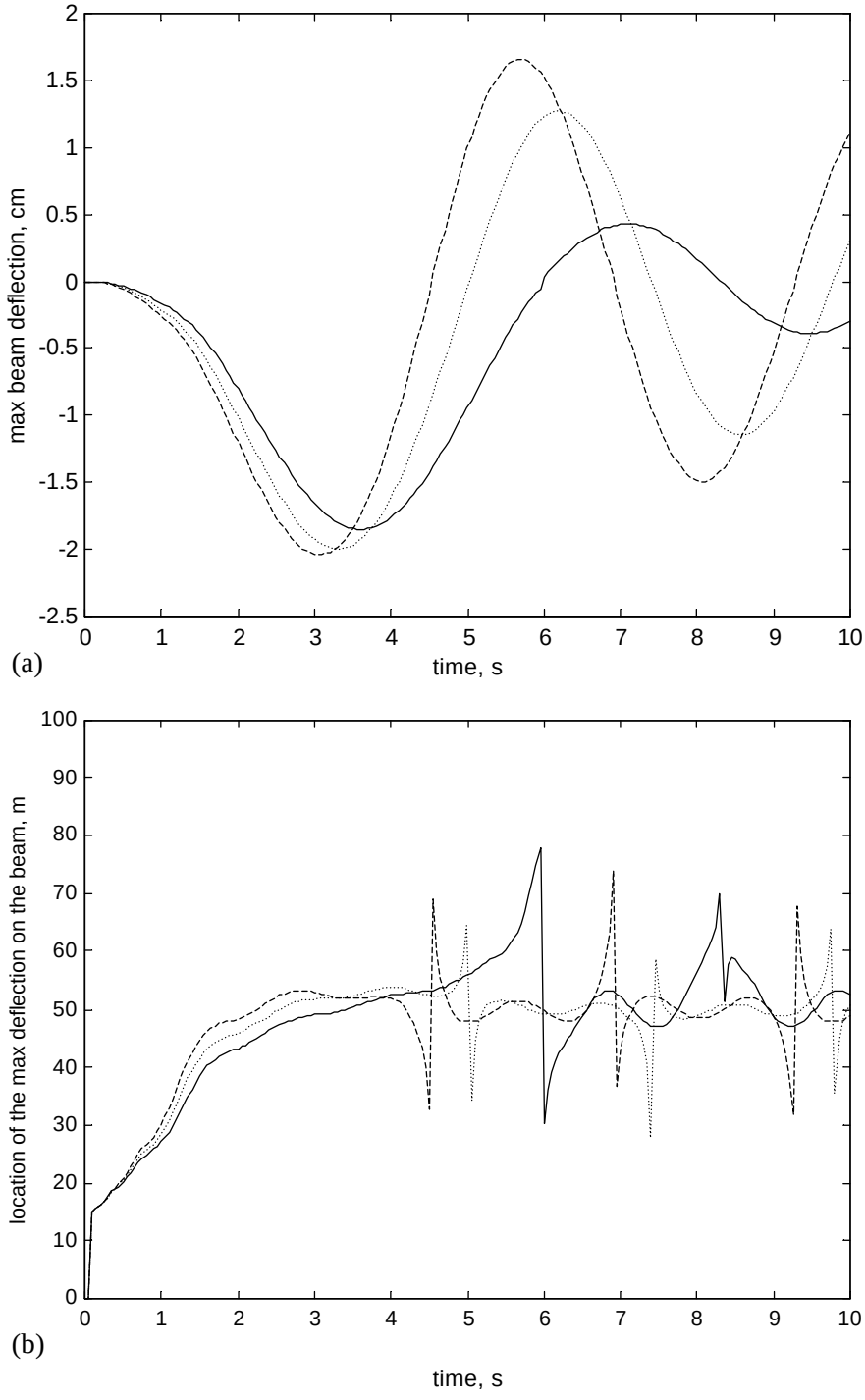

Fig. 11. Maximum dynamic (a) beam diflection and (b) location for $V = 56$ (—), $V = 72$ (. . . .), and $V = 88$ km/h (- - -).

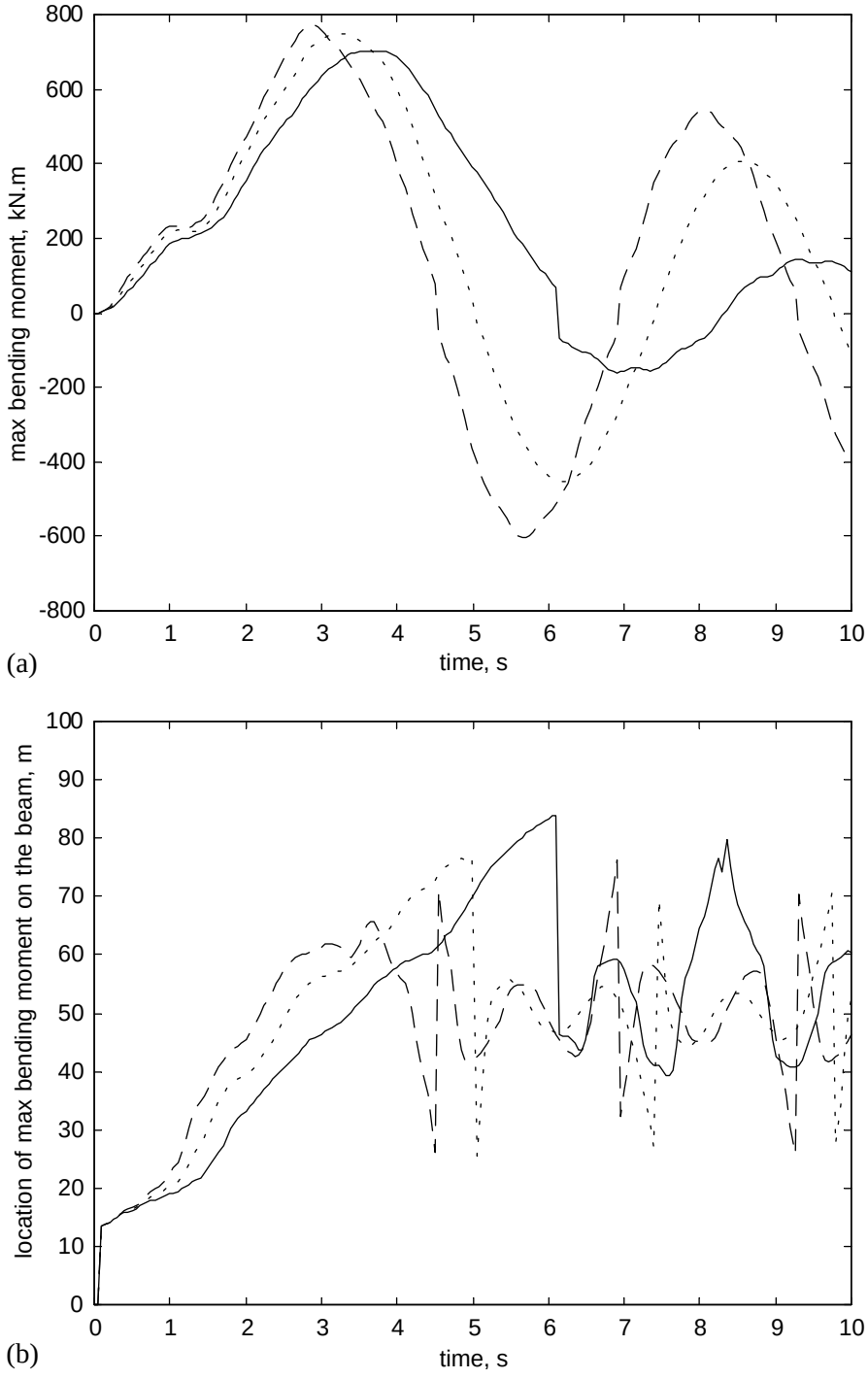

Fig. 12. (a) Maximum bending moment and (b) location for $V = 56$ (—), $V = 72$ (. . . .), and $V = 88$ km/h (- - -).

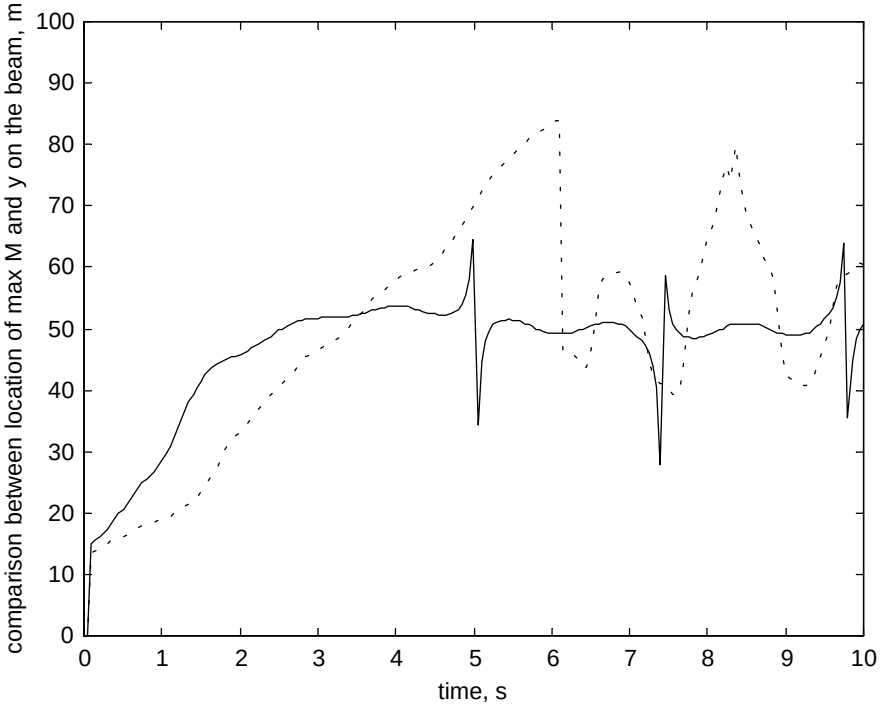

Fig. 13. Comparison between maximum deflection location and bending moment location for $V = 56$ km/h, deflection (—) and bending moment (- - -).

respectively. Furthermore, the maximum value of $\mathbf{y}^{x}_{max}$, found over different instants of time, will render the same maximum values (i.e., $y_{max\,max}$) but with different index, representing the corresponding instant of time, which is referred to as $t_{max\,max}$. Using this instant of time, the position of the center of gravity of the vehicle can be determined and noted as $x_{max\,c.g}$.

(4) The vehicle speed is now varied over the prescribed interval, for instance $V \in [40, 120]$ km/h, and steps (1)–(3) are then repeated to reveal the variations of $y_{max\,max}$, $x_{max\,max}$, and $x_{max\,c.g}$ with respect to the changes in the vehicle speed.

Similar procedure can be followed for the study of the bending moment M_b of the bridge structure. The variations of the maximum value of the transversal dynamic deflection and the bridge bending moment, with respect to the vehicle speed, are shown in Figs. 14 and 15, respectively. It is observed that when the vehicle travels at 91.2 km/h the parameter $y_{max\,max}$ attains its maximum value, and therefore, it can be referred to as the critical speed of the vehicle corresponding to the maximum transversal deflection.

This critical velocity is slightly reduced (88 km/h) for the maximum value of the bending moment, as shown in Fig. 15. It is interesting to note that the maximum value of the dynamic deflection occurs almost at the mid-span of the bridge (with $\pm 3\%$ variations), as illustrated in Fig. 14(b), while, the maximum value of the bending moment occurs at a farther vicinity of the mid-span ($\pm 20\%$), as seen from Fig. 15(b). Moreover, as the vehicle speed increases the time that corresponds to the position of the center of gravity of the vehicle increases accordingly. For

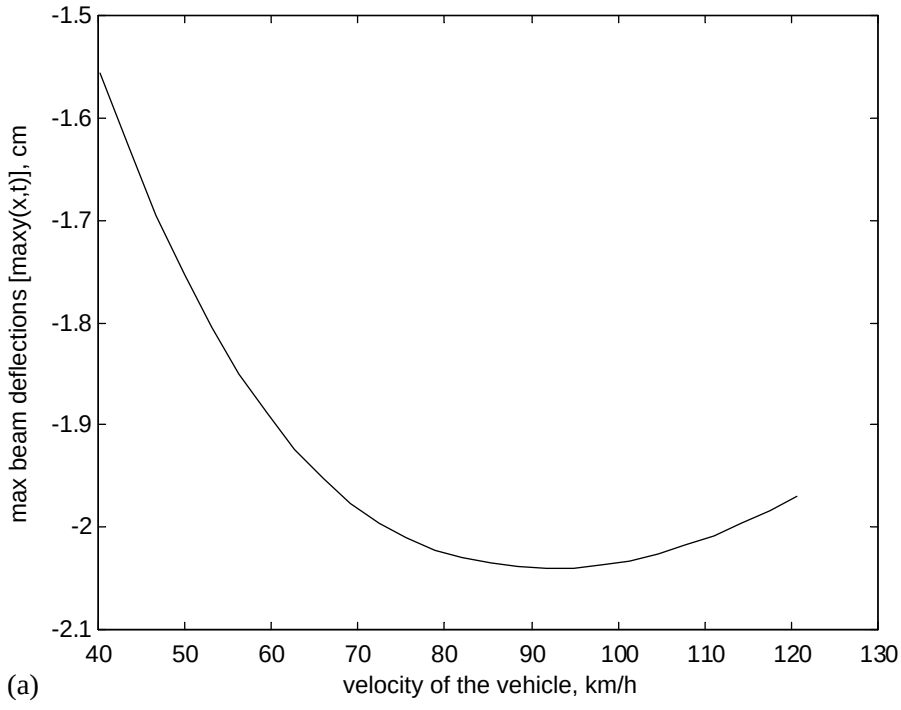

(a)

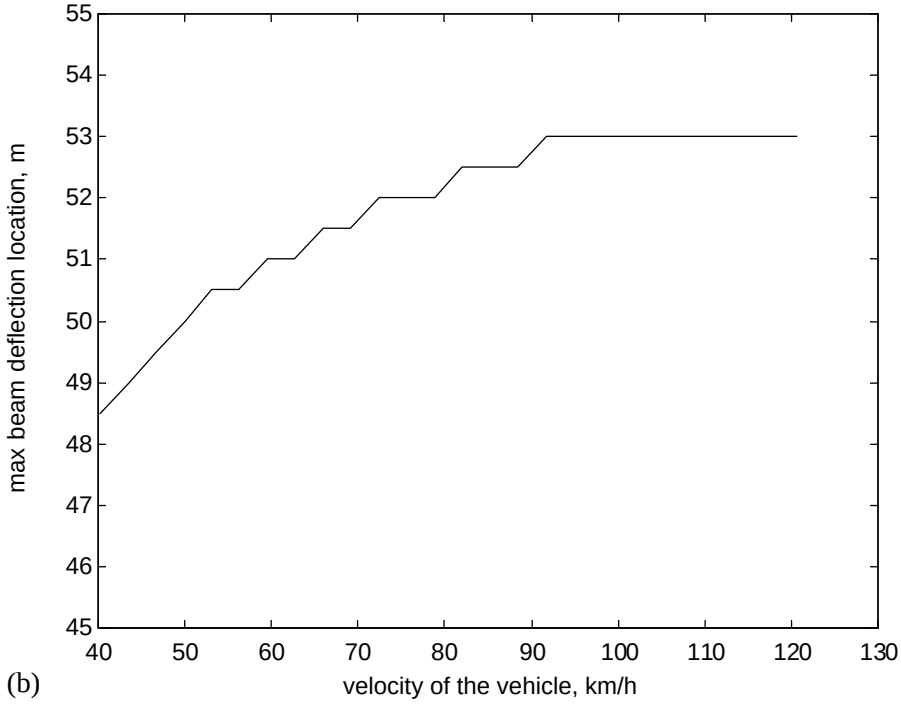

(b)

Fig. 14. (a) The maximum dynamic deflection and (b) location versus vehicle velocity.

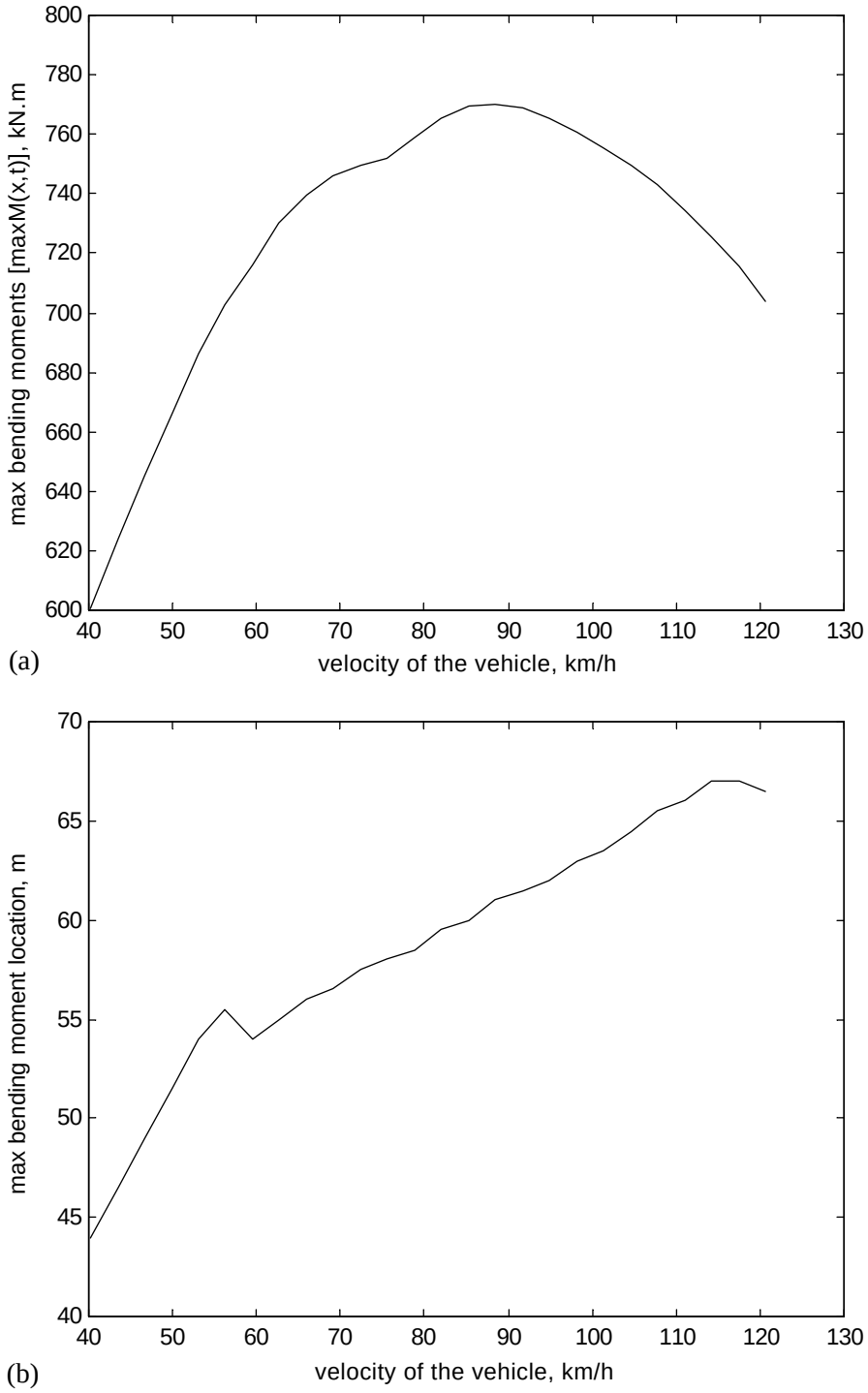

Fig. 15. (a) The maximum bending moment and (b) location versus vehicle velocity.

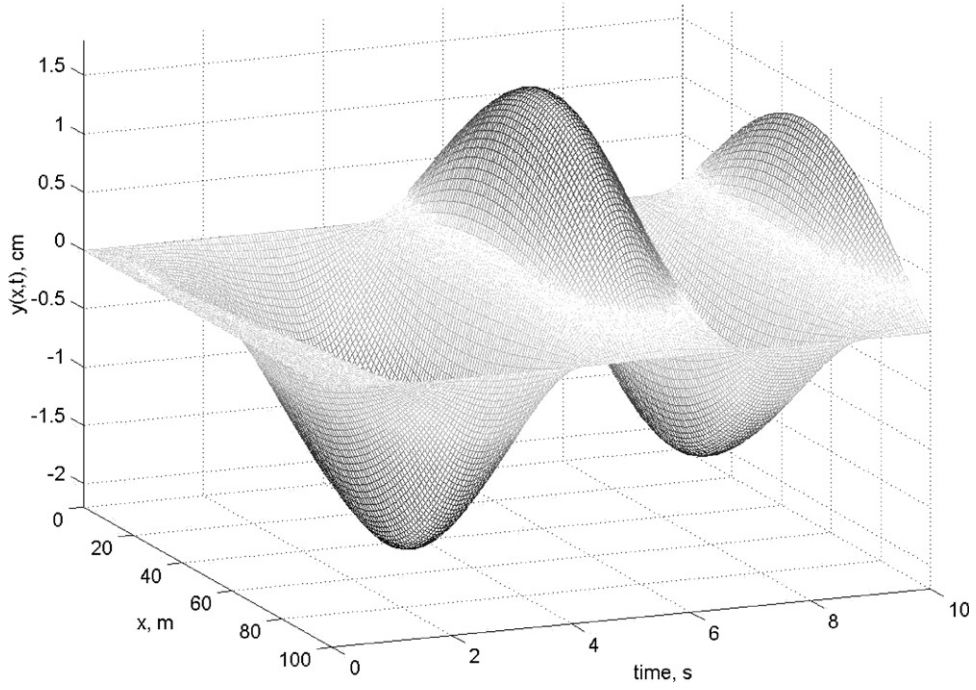

Fig. 16. Waterfall effect of dynamic deflection for $V = 91.2\,\text{km/h}$ (critical velocity).

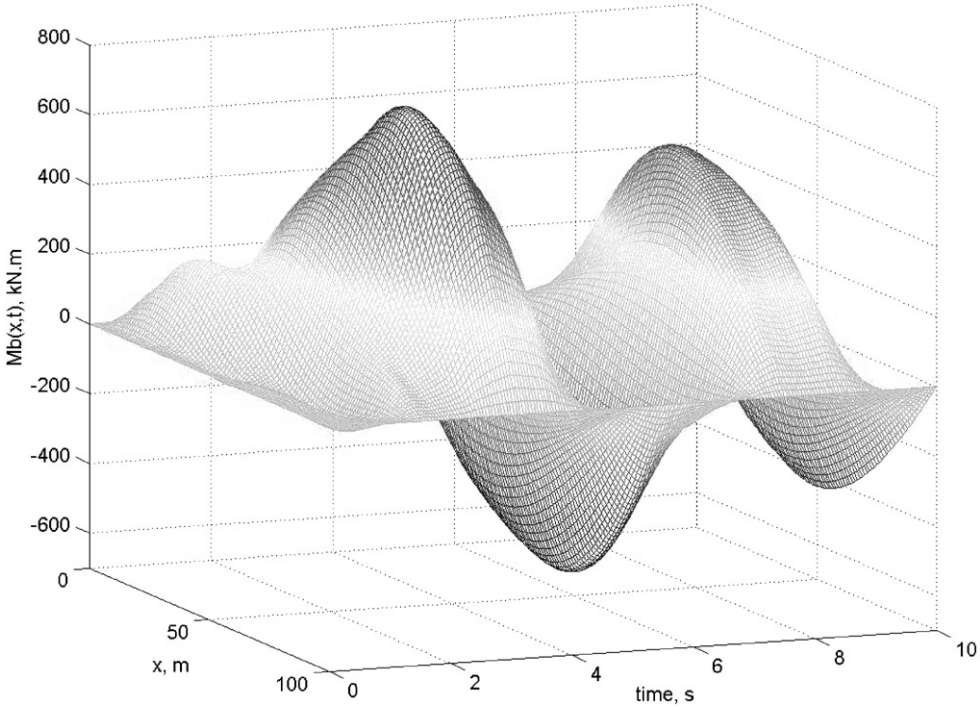

Fig. 17. Waterfall effect of bending moment for $V = 91.2\,\text{km/h}$ (critical velocity).

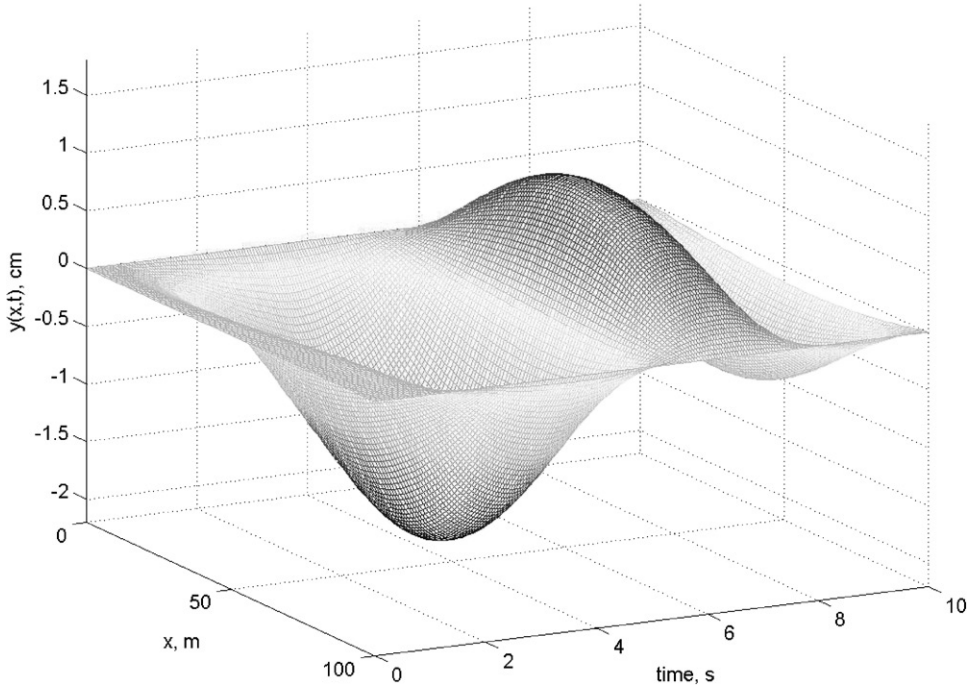

Fig. 18. Waterfall effect of dynamic deflection for $V = 64$ km/h (non-critical velocity).

instance, when the vehicle travels at 48 km/h the maximum deflection occurs when the vehicle is situated at the mid-span and almost at the most right end of the bridge when it travels at 120 km/h.

An attempt is now made to present the time trace of the transversal deflection of every point along the bridge and the structural bending moment of the bridge using a waterfall depiction. Figs. 16 and 17 illustrate the waterfall for the transversal dynamic deflection of the bridge, $y(x, t)$, and the values of the bending moment, $M_b(x, t)$, respectively, as the vehicle travels at its critical speed ($V = 91.2$ km/h). Finally, a somewhat arbitrary value of the speed other than the critical value, say $V = 64$ km/h, has been chosen and the waterfall depictions of the transversal dynamic deflection and the bending moment values are presented in Figs. 18 and 19, respectively.

6. Conclusions

The vehicle–structure interaction problem of a bridge traversed by a moving vehicle has been investigated. The vehicle including the occupants was modelled as a half-car planar model with six degrees-of-freedom, and the bridge was assumed as an Euler–Bernoulli beam. The relationship between the bridge vibration characteristics and the vehicle speed was determined, which resulted into a search for a particular speed that determined the maximum values of dynamic deflection and the bending moment of the bridge. Results at different vehicle speeds demonstrated that the maximum dynamic deflection occurs at the vicinity of the bridge mid-span ($\pm 3\%$), while the

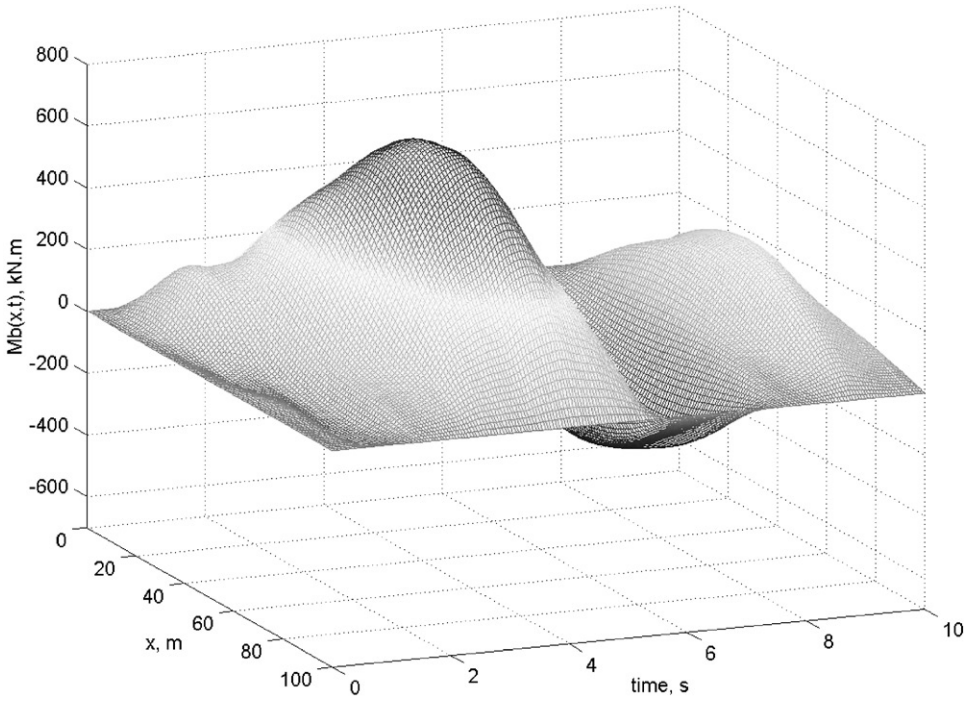

Fig. 19. Waterfall effect of bending moment for $V = 64\,\text{km/h}$ (non-critical velocity).

maximum bending moment was found to be at $\pm 20\%$ of the mid-span. Additionally, it was shown that the use of SQC model does not provide adequate information for both vehicle dynamics and bridge characteristics, when compared with the half-car model.

References

[1] G.G. Stokes, Discussion of a differential equation relating to the breaking of railway bridges, Transactions of the Cambridge Philosophical Society, Part 5 85 (1849) 707–735.
[2] R. Willis, Commissioners report: application of iron to railway structures, William Clowes & Sons, London, 1849.
[3] S. Timoshenko, On the forced vibration of bridges, Philosophical Magazine Series 6 (43) (1922) 1018.
[4] R.S. Ayre, G. Ford, L.S. Jacobsen, Transverse vibration of a two span beam under the action of a moving constant force, American Society of Mechanical Engineers Transactions, Journal of Applied Mechanics 17 (1950) 1–12.
[5] A.N. Krylov, Mathematical Collection of Papers of the Academy of Sciences, Vol. 61, 1905, St. Petersburg, Russia.
[6] A.N. Krylov, Über die erzwungenen Schwingungen von gleichformigen elastischen Staben, Mathematische Annalen 61 (1905) 211.
[7] C.E. Inglis, A Mathematical Treatise on Vibration in Railway Bridges, Cambridge University Press, Cambridge, 1934.
[8] L. Fryba, Vibration of Solids and Structures Under Moving Loads, Telford, London, 1999.
[9] S. Timoshenko, D.H. Young, W. Weaver, Vibration Problems in Engineering, 4th Edition, Wiley, New York, 1974.
[10] G.B. Warburton, The Dynamic Behaviour of Structures, Pergamon Press, Oxford, 1976.

[11] F.V. Hilho, Finite element analysis of structures under moving loads, Shock and Vibration Digest 10 (1978) 27–35.
[12] J. Hino, T. Yoshimura, K. Konishi, A finite element method prediction of the vibration of a bridge subjected to a moving vehicle load, Journal of Sound and Vibration 96 (1986) 45–53.
[13] S. Sadiku, H.H.E. Leipholz, On the dynamics of elastic systems with moving concentrated masses, Ingenieur-Archiv 57 (1987) 223–242.
[14] R. Katz, C.W. Lee, A.G. Ulsoy, R.A. Scott, The dynamic response of a rotating shaft subject to a moving load, Journal of Sound and Vibration 122 (1988) 131–148.
[15] S.C. Huang, J.S. Chen, Dynamic response of spinning orthotropic beams subjected to moving harmonic forces, Journal of the Chinese Society of Mechanical Engineers 11 (1990) 63–73.
[16] E. Esmailzadeh, M. Ghorashi, Dynamic behavior of vehicles traveling on bridges, Proceedings of the 14th Biennial ASME Conference on Vibration and Noise, DE 63, Sept. 19–22, 1993, Alburguerque, NM, pp. 133–139.
[17] E. Esmailzadeh, M. Ghorashi, Vibration analysis of beams traversed by uniform partially distributed moving masses, Journal of Sound and Vibration 184 (1) (1995) 9–17.
[18] E. Esmailzadeh, M. Ghorashi, Vibration analysis of Timoshenko beams subjected to a traveling mass, Journal of Sound and Vibration 199 (4) (1997) 615–628.
[19] R.T. Wang, Vibration of multi-span Timoshenko beams subjected to a moving force, Journal of Sound and Vibration 207 (1997) 731–742.
[20] H.P. Lee, Dynamic response of a beam with intermediate point constraints subject to a moving load, Journal of Sound and Vibration 171 (1994) 361–368.
[21] D.Y. Zheng, Y.K. Cheung, F.T.K. Au, Y.S. Cheng, Vibration of multi-span non-uniform beams under moving loads by using modified beam vibration functions, Journal of Sound and Vibration 212 (1998) 455–467.
[22] J.S. Wu, C.W. Dai, Dynamic response of multi-span non-uniform beams due to moving loads, Journal of Structural Engineering 113 (1987) 458–474.
[23] K. Henchi, M. Fafard, Dynamic behavior of multi-span beams under moving loads, Journal of Sound and Vibration 199 (1997) 33–50.
[24] D.J. Inman, Engineering Vibration, 2nd Edition, Prentice-Hall, Englewood Cliffs, NJ, 2001.
[25] N. Olgac, N. Jalili, Modal analysis of flexible beams with delayed resonator vibration absorber: theory and experiment, Journal of Sound and Vibration 218 (1998) 307–331.
[26] Matlab/Simulink, Version 5.3, Release R11, The MathWorks Inc., Natick, MA, 1999.
[27] Maple, Waterloo Maple Inc., Waterloo, Ontario, 2000.